Design of a Switching Nonlinear MPC for Emission Aware Ecodriving

Gian Paolo Incremona, *Member, IEEE*, and Philipp Polterauer

***Abstract*—Advanced automation and information systems are shaping the future of transportation by enabling advanced approaches, such as ecodriving control strategies, which improve safety and energy efficiency of personal transport. This paper contributes to the field of ecodriving control by developing a novel approach capable to deal with curvy roads, combining road grade and curvature look ahead to keep the driving comfortable, while also considering pollutant emissions. The formulation and solution of emission aware ecodriving as an optimal control problem is presented and, more specifically, a novel switching Nonlinear Model Predictive Control (NMPC) is proposed. Its feasibility and potential are shown by means of simulation case studies based on real world test cases, a validated vehicle model, and measured road topology. Hence, it is shown that emission aware ecodriving is a viable option and that developers of future ecodriving systems should expand their focus from solely energy efficiency towards additional targets.**

***Index Terms*—Energy efficiency, emission control, optimal control, vehicle dynamics.**

I. Introduction

EMISSIONS from exhaust gas, especially those produced by conventional road vehicles, have been and still are in the focus of research and legislation changes, due to the various negative effects on human health [1]. Specifically, many factors can affect fuel consumption and emissions, such as the engine type, power-train systems or road characteristics as shown for instance in [2], [3] among many other works. Yet, beside these factors, as shown in [4] or also by more recent studies such as [5], a substantial, and often overlooked factor is the driver himself, and fixed procedures for certification do not help in alleviating this influence. Therefore, there have been non control based approaches, referred to as ecodriving, where training and guidelines for drivers are applied, which are usually based on heuristic [5], [6], in order to improve the driving skills and sensitize people to lead them to more efficient driving. However, some studies, e.g., [7], investigated the impact of these ecodriving guidelines on nitrogen oxides (NO_x) emissions and found no significant improvement, therefore motivating further studies on emission aware ecodriving.

This is the final version of the paper accepted for publication in IEEE Transactions on Intelligent Vehicles, doi: 10.1109/TIV.2022.3140484. This work has been partially supported by the Italian Ministry for Research in the framework of the 2017 Program for Research Projects of National Interest (PRIN), Grant no. 2017YKXYXJ. G. P. Incremona is with the Dipartimento di Elettronica, Informazione e Bioingegneria (DEIB), Politecnico di Milano, Piazza Leonardo da Vinci 32, 20133 Milan, Italy (e-mail: *gianpaolo.incremona@polimi.it*).

P. Polterauer is with MAGNA Engineering Center Steyr, and was with the Institute for Design and Control of Mechatronical Systems, Johannes Kepler University Linz, Altenbergerstraße 69, 4040 Linz, Austria (e-mail: *philipp.polterauer@jku.at*).

Fortunately, due to the advances in sensing and control technology [8], [9], the development of autonomous vehicles and Advanced Driver Assistance Systems (ADAS) has gained momentum and has seen substantial improvements. While the main objectives of such systems are typically safety and comfort, other driving objectives such as energy consumption and emissions can be improved as well. Due to computational power getting cheaper, advanced control strategies aiming to maximize energy efficiency of vehicle driving, commonly referred to as ecodriving control, are enabled. In ecodriving control, for conventional vehicles, the objective is to reduce the fuel consumption by finding appropriate control sequences. Depending on the model's level of detail, this can be either sequences for gas and brake pedal or intermediate substitute variables such as acceleration or torques. Ecodriving control is not limited to on road vehicles. Indeed, ecodriving control problems or related optimal control problems have been studied in other settings as well, e.g., efficient operation of trains [10], [11] or ecoflying in aircraft [12]. In this paper we study ecodriving control of road classical vehicles, in particular passenger cars with conventional engines. Therefore, the term ecodriving, although used in many domains, from here on is used as a short hand for the efficient operation of the longitudinal dynamics of a conventional vehicle.

More specifically, we focus our attention on pollutant emissions, thus extending previous results dealing solely with fuel consumption and energy efficiency targets. To pursue this objective, a NMPC is designed relying on the optimal operation of a conventional vehicle described by the combination of four different modes, i.e., acceleration, cruising, coasting and braking [13]. Since using switching NMPC in its original formulation can be very difficult, in order to satisfy the computational requirements enforced by proprietary software in physical vehicle employed in an automotive setting, some technical measures and improvements have been also introduced, thus making the proposal eligible to be applied in field implementations.

A. Comparison with related works on ecodriving

The literature about ecodriving control is rich and a good overview of the ecodriving control problems and how they can be solved is given in [13], where some insights into the solution methods and drawbacks are given. If the ecodriving is approached through formulation and solution of an optimal control problem, the most used method is Dynamic Programming (DP). Although DP has significant drawbacks, the ecodriving problem can usually be solved effectively with it.

There are two main reasons for that: first the models typically used in ecodriving do not contain many states, usually they are two or maximum three, and second the nonlinearity which is present in the efficiency characteristics of conventional engines can easily be considered. Besides DP, which is typically applied offline, other solution approaches are employed but they typically need reformulation and approximation of the original problem [14]–[16].

Gear shifting, although crucial for maximizing efficiency, is often not considered in the ecodriving control (see [16]–[18]). Some solutions aimed at finding both the optimal velocity profile and the best engine torque and gear position, are instead proposed for instance in [19]–[23]. More commonly, it is found in heavy duty applications, since the gear shifting time is typically significantly longer than in passenger cars. The authors of [19], [20] propose, for instance, a DP based control approach which operates on a small horizon in order to reduce the computational complexity and they pay special attention to the modelling of the gear shifting process. No lateral dynamics are considered, and simulations are performed for a motorway route. In the literature, road grade and speed limits are considered quite frequently, but a curve aware ecodriving can be found in a handful of works, [24], [25].

Reducing emissions represents another important challenge in the automobile industry which has to balance the conflicting objectives of improving fuel economy and fulfilling constraints on exhaust production. This problem typically results in poor driveability and optimal automotive control proposals date back to the 1980s (see, e.g., [26] and the references therein). Typically, exhaust emissions are tackled after they have been produced and only few references consider emissions included in the ecodriving control problem formulation. In [27], for instance, a solely fuel optimal control problem considering road slopes is solved via DP to generate eco-speed profile. Traffic conditions for fuel efficient driving by optimizing the speed profile are instead considered in [28], while in [29] a Model Predictive Control (MPC) is adopted to get an optimal speed trajectory, by taking into account, implicitly in the cost, the factors influencing fuel consumption and emissions. In [30] two ecodriving control problems are formulated and solved. In the first one the total fuel consumption is considered as the objective, while in the second one, the so-called ecological driving problem, an emission penalty is instead introduced. In fact, pollutants are not explicitly considered but introduced as a high torque penalty since this area is shown to be producing high emissions. In the recent work [17], a more rigorous approach is introduced, resulting in an emission aware ecodriving control utilizing a dynamical model for emission aftertreatment system, but with optimal profiles under emission consideration being very different from the pure fuel optimal case. In [31] the effect of lateral acceleration limits on optimal solutions to multi-objective ecodriving is investigated, evaluating the role of longitudinal acceleration with respect to NO_x emissions. In the recent work [32], the inclusion of terminal constraints in the cost function allows to investigate the optimal trade-off between NO_x and fuelling.

B. Contributions

In this paper we put forward an alternative ecodriving control approach, which actively accounts for NO_x emissions in their production phase. It is partially based and extends the results of the Ph.D. thesis [33] and of the preliminary work [34], where a classical ecodriving control problem is solved without taking into account the presence of emissions. Specifically, this work addresses the design of an emission aware ecodriving control problem, which is recast as a nonlinear switching multivariable Optimal Control Problem (OCP). Exploiting the modelling assumptions given in [13] indeed makes the vehicle model switching and therefore motivates the use of a switching NMPC (see [35]–[38] for stability and stabilization results of switching systems).

The merit of this article, apart from proposing a new switching NMPC strategy, is the investigation of its performance with respect to DP, which naturally represents the optimal solution to the ecodriving problem. Although, as expected, a reduction in the performance can be observed, the proposed NMPC simplifies the problem and represents a valid real time ready-to-implement solution. Therefore, another contribution of the work is to provide a deep simulation assessment of the proposal relying on real data, also giving tuning practices for practitioners who wish to implement similar approaches on the field. To this scope, some modifications on the genuine NMPC are also introduced, such as a minimum time based precomputation of velocity limits to improve the feasibility of the algorithm in the case of short prediction horizons. Finally, we want to stress that, differently from DP, our approach does not suffer the curse of dimensionality, meaning that it can be extended to more complex models (e.g., other dynamic emissions models) without a big impact on the execution time.

The paper is organized as follows. In Section II some preliminaries on switching NMPC are recalled. In Section III the vehicle model is described and the control problem is formulated. The proposed NMPC algorithm is discussed in Section IV, while simulations carried out on a realistic case study are reported in Section V. Some conclusions are drawn in Section VI. In Appendices A and B the parametrization and validation of the vehicle model are given.

Notation

The used variables and operators are mostly standard, but some notation needed for MPC is introduced. Let z be a vector, then z_i refers to its ith entry. Given a signal z, then $z_{p|k}$ denotes its prediction at point p, predicted at the time k, so that, at the prediction time instant k one has $z_{k|k} = z_k$. Moreover, let N_p be the horizon length, $\mathcal{K}_k = \{k, .., k + N_\mathrm{p} - 1\}$ be the set of prediction steps, $\mathbf{u}_k := u_{[k,k+N_\mathrm{p}-1|k]} = u_{\mathcal{K}_k|k}$ be the whole input sequence from k to $k + N_\mathrm{p} - 1$, and $\mathbf{x}_k := x_{\mathcal{K}_k|k}$ the whole state sequence from k to $k + N_\mathrm{p}$, both predicted at time k.

II. Some Preliminary Issues

The so-called Switching Nonlinear Model Predictive Control (SNMPC), obtained by solving the Switching Finite Horizon Optimal Control Problem (SFHOCP) in a receding horizon fashion, is presented below.

Consider the discrete-time switched nonlinear system

$$x_{k+1} = f_{\sigma_k}(x_k, k), \quad \forall\, k \in \mathbb{N}, \tag{1}$$

where $x \in \mathbb{R}^n$ is the state, while $\sigma_k \in \mathbb{N}$ is the switching command. The active model at the time instant k is determined by the integer $\sigma_k \in \mathcal{S}$, with $\mathcal{S} = \{1, \cdots, M\}$. The SFHOCP, where the aim is to minimize a predefined cost $J_{\mathbf{w}}$ with respect to the switching sequence $\mathbf{w}_k = w_{[k,k+N_\mathrm{p}-1|k]} = [\sigma_{k|k}, \ldots, \sigma_{k+N_\mathrm{p}-1|k}]$, is defined as

$$\begin{aligned} \min_{\mathbf{w}_k} J_{\mathbf{w}} &= \sum_{p\in\mathcal{K}_k} g_{\sigma_p}(x_{p|k}, p) + h(x_{k+N_\mathrm{p}|k}) \\ \text{s. t.} \quad x_{p+1|k} &= f_{\sigma_{p|k}}(x_{p|k}, p) \\ x_{p|k} &\in \mathcal{X} \\ x_{k+N_\mathrm{p}|k} &\in \mathcal{X}_\mathrm{f} \\ x_{k|k} &= x_k, \end{aligned} \Bigg\} \forall p \in \mathcal{K}_k \tag{SFHOCP}$$

where $x_{p|k}$ depends on the switching strategy $\mathbf{w}_k$ over the prediction horizon, $\mathcal{X} \subset \mathbb{R}^n$ is the state constraint set and $\mathcal{X}_\mathrm{f} \subset \mathbb{R}^n$ is the terminal constraint set.

At each sampling instant k, the optimal switching policy, denoted by $\mathbf{w}^\mathrm{o}_{[k,k+N_p-1|k]} := [\sigma^\mathrm{o}_k, \ldots, \sigma^\mathrm{o}_{k+N_\mathrm{p}-1}]$ is inside the set of feasible sequences $\mathcal{F}_k \subseteq \mathcal{W}_k$, which itself is a subset of all possible sequences $\mathcal{W}_k$. A sequence $\mathbf{w}_k$ is called feasible if all constraints are satisfied along the horizon, i.e.,

$$\mathcal{F}_k := \left\{ \mathbf{w}_k \in \mathcal{W}_k : x_{p|k} \in \mathcal{X} \quad \forall p \in \mathcal{K}_k \ \wedge\ x_{k+N_\mathrm{p}|k} \in \mathcal{X}_\mathrm{f} \right\}. \tag{2}$$

Since the input can only assume a finite number of values, a countable number of possible input sequences, represented by $\mathcal{W}_k$, exists. Therefore, a solution to (SFHOCP) can be found using a brute force procedure as outlined in the following. Note that, although the Bellman's principle of optimality could be used to reduce the number of combinations, the brute-force approach allows us to parallelize the optimization thus getting faster results, more suitable for field implementations.

For each sequence $\mathbf{w}_i$ in the set of all possible sequences $\mathcal{W}_k$, the switched system dynamics are simulated. The simulation is easily obtained by repeatedly evaluating (1). The outcome of this simulation is either infeasibility of the sequence (if along the simulation a constraint from the SFHOCP is violated) or, if the sequence is feasible, the corresponding cost function value $J_{\mathbf{w}_i}$. After all sequences have been simulated, a cost value is available for each feasible sequence. Then the optimal sequence is found as the minimal value among these cost values. From the corresponding optimal sequence the input value at the first time instant is selected to be applied to the system.

For the previous procedure, we measure the computational complexity by the number of evaluations N_f of the dynamics function $f_{\sigma_p|k}$, that have to be performed for computing the optimal sequence. For each sequence $\mathbf{w}_k \in \mathcal{W}_k$ the dynamics is simulated along the horizon leading to $N_\mathrm{p} - 1$ evaluations for each sequence. The number of sequences in $\mathcal{W}_k$ is equal to the cardinality of the set, and, due to the combinatorial nature of the strategy, the cardinality of $\mathcal{W}_k$ is given by $\mathrm{card}\,\mathcal{W}_k = M^{N_\mathrm{p}}$, so that $N_f = (N_\mathrm{p}-1)\cdot M^{N_\mathrm{p}}$. It follows that two factors, $\mathrm{card}\mathcal{W}_k$ and N_p, influence the computational complexity.

III. Problem Setting

Now, we present the vehicle model, which is used in the following sections dealing with the ecodriving control problem. Since energy demand is mostly effected by the longitudinal control of a vehicle, a model of the longitudinal dynamics is developed for the case of a conventional vehicle on a curvy road. Lateral dynamics is defined through the curvature of the route and the velocity. For the sake of clarity, all the parameters used in the following are also summarized in Table I.

Table I: Parameters nomenclature.

m	vehicle mass
m_eff	effective mass
g	gravitational constant
A	front area of the vehicle
r	wheel radius
ρ_air	density of air
c_r	rolling resistance
c_d	drag coefficient
η	driveline and gearbox efficiency
λ	rotational inertia factor
s_f	end point of the trip
t_f	final time
v_max	velocity limit
j_max	maximum gear
$a_\mathrm{x,min/max}$	longitudinal acceleration limits
$a_\mathrm{y,min/max}$	lateral acceleration limits
$\tau_\mathrm{b,min/max}$	braking torques limits
$\omega_\mathrm{e,min/max}$	engine speed limits
$\tau_\mathrm{e,min/max}$	engine torque limits
$N_\mathrm{gs,max}$	maximum number of gearshifts
$m_{\mathrm{NO_x},\mathrm{max}}$	emission constraints
μ_gs	weight on the number of gearshifts
$\mu_{\mathrm{NO_x}}$	weight on the $\mathrm{NO_x}$ emission
μ_{t_f}	weight on the travel time
N_p	prediction horizon
N_b	number of blocks over the horizon

A. Road model

First of all, the road of length s_f is modelled as a collection of three position s dependent functions: i) $c(s) : [0,\, s_\mathrm{f}] \to \mathbb{R}$ is the curvature function which characterizes the curves of the route and influences the lateral acceleration; ii) $\phi(s) : [0,\, s_\mathrm{f}] \to \mathbb{R}$ is the road grade angle which describes the steepness of the road and influences mainly the climbing force; iii) $v_\mathrm{max}(s) : [0,\, s_\mathrm{f}] \to \mathbb{R}$ describes the maximum velocity allowed along the route.

B. Vehicle model

The vehicle dynamics (on a route) are described in continuous-time through the two dimensional system

$$\dot{s} = v \tag{3}$$

$$\dot{v} = \tfrac{1}{m_\mathrm{eff}} \left[F_\mathrm{t} - F_\mathrm{r}(s, v) \right], \tag{4}$$

where s is the position of the vehicle on the road, v is the velocity, F_t is the traction force and F_r is the resistance force.

1) Resistance force: The term F_r typically consists of three parts: a rolling F_roll, a climbing F_grade and a drag F_drag resistance, [39], that is

$$F_\mathrm{r}(s, v) = F_\mathrm{roll} + F_\mathrm{grade}(s) + F_\mathrm{drag}(v). \tag{5}$$

The rolling resistance F_roll is given as

$$F_\mathrm{roll} = mgc_\mathrm{r}. \tag{6}$$

The downhill force F_{grade} is given by

$$F_{\text{grade}}(s) = mg\sin(\phi), \tag{7}$$

whereas the aerodynamic drag force F_{drag} is

$$F_{\text{drag}}(v) = \frac{c_{\text{d}}\rho_{\text{air}}A}{2}v^2. \tag{8}$$

Combining the definitions above leads to

$$F_{\text{r}}(s,v) = mg\left(\sin(\phi(s)) + c_{\text{r}}\right) + \frac{c_{\text{d}}\rho A}{2}v^2, \tag{9}$$

where m is the vehicle mass, g the gravitational constant, a_{x} is the longitudinal acceleration, $\sin(\phi)$ is the road grade, ρ_{air} the density of air, A the front area of the vehicle, c_{r} the rolling resistance and c_{d} the drag coefficient.

2) Lateral acceleration: The lateral acceleration for a known route is given by

$$a_{\text{y}}(s,v) = v^2 \cdot c(s), \tag{10}$$

where $c(s)$ is the curvature of the route. Although we mainly focus on the longitudinal control, we consider the lateral acceleration in order to limit the vehicle driving for comfortable accelerations.

3) Wheel: We consider a stiff wheel with perfect rolling (no slip), and we assume the rolling resistance to be included in the vehicle resistance. The wheel model is given by the following algebraic relations

$$\omega_{\text{w}} = \frac{v}{r} \tag{11}$$

$$F_{\text{t}} = \frac{1}{r}\left(\tau_{\text{pt}} - \tau_{\text{b}}\right), \tag{12}$$

where τ_{pt} and τ_{b} are the gearbox torque and braking torque, respectively, and r the wheel radius.

4) Brakes: We assume the braking system to be much faster than the vehicle dynamics and it is henceforth neglected. In our model the brake input is just the actual brake torque $u_b = \tau_{\text{b}}$. We further assume that $\tau_{\text{b}} \in [\tau_{\text{b,min}}, \tau_{\text{b,max}}]$, where $\tau_{\text{b,min}}$ is assumed to be typically zero and $\tau_{\text{b,max}}$ is a parameter of the model.

5) Converter and clutch: The clutch open and gear speed adoption phase are neglected, so that one has $\tau_{\text{c}} = \tau_{\text{e}}$ and $\omega_{\text{c}} = \omega_{\text{e}}$, with τ_{c}, ω_{c} and τ_{e}, ω_{e} being torque and rotational velocity of clutch and engine, respectively.

6) Gearbox and driveline: The gearbox is modelled as a dynamic system with a discrete state j, influenced by the switching signal $u_{\text{g}}(t) \in \{-1, 0, 1\}, \forall t \in [t_0, t_{\text{f}}]$. The update equation is

$$j^+(t) = j(t) + u_{\text{g}}(t), \quad \forall t \in T_j. \tag{13}$$

The set of gear switching times T_j is defined as $T_j := \{t \in [t_0, t_{\text{f}}] : u_{\text{g}}(t) \neq 0\}$. The total number of gearshifts is then given by the cardinality of the set T_j, i.e., $\#_{\text{GS}} = \text{card}(T_j)$. The gearbox model additionally includes the state dependent algebraic relations

$$\omega_{\text{e}} = \gamma^{(j)} \cdot \omega_{\text{w}} \tag{14}$$

$$\tau_{\text{pt}} = \eta^{\text{sign}(\tau_{\text{c}})}\gamma^{(j)} \cdot \tau_{\text{c}}, \tag{15}$$

where η is the driveline and gearbox efficiency (usually assumed constant for all gears), $j \in \{1, ..., j_{\text{max}}\}$ is the current gear and $\gamma^{(1)}, ..., \gamma^{(j_{\text{max}})}$ are the set of transmission ratios.

7) Rotational inertias: Since the gearbox and the wheel are modelled through static relations of the speeds, the rotational inertias from engine to wheel can be modelled as one big inertia, for a constant gear. This is done by introducing an equivalence factor λ on the vehicle mass, i.e., $m_{\text{eff}} = \lambda^{(j)} \cdot m$, where m_{eff} is the effective mass in (4), m is the vehicle mass and λ the factor accounting for the rotational inertia. As the value of λ depends on the engaged gear j, the notation $\lambda^{(j)}$ is used.

8) Engine: We model the engine as a static system, which means that there is an algebraic relation between the engine speed ω_{e}, fuel consumption q_{fuel} and the engine torque τ_{e}. More specifically, taking also into account the emission flow q_{NO_x}, we refer to the so-called static backward engine model

$$q_{\text{fuel}} = f_{\text{fuel}}(\omega_{\text{e}}, \tau_{\text{e}}) \tag{16}$$

$$q_{\text{NO}_\text{x}} = f_{\text{NO}_\text{x}}(\omega_{\text{e}}, \tau_{\text{e}}). \tag{17}$$

Note that, in this paper, we have considered only NO_x emissions as these are the most relevant ones for Diesel engines. The approach could be however extended to other emissions that do not necessarily need to be modelled in the same way. Furthermore, the engine operation is limited to a domain

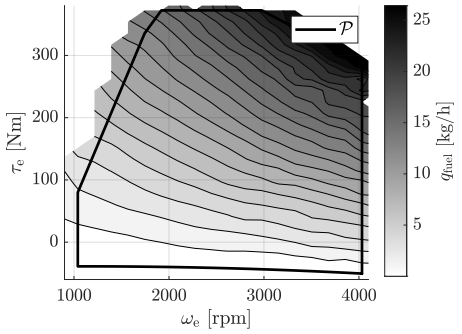

(a) $q_{\text{fuel}} : \mathcal{P} \to \mathbb{R}^+$

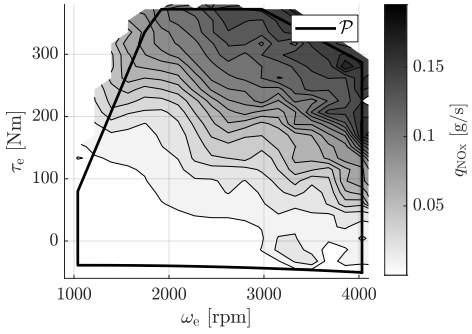

(b) $q_{\text{NO}_\text{x}} : \mathcal{P} \to \mathbb{R}^+$

Figure 1: Static engine operating point in the region $\mathcal{P}$ (solid line) for fuel consumption and NO_x emission.

denoted $(\omega_{\text{e}}, \tau_{\text{e}}) \in \mathcal{P}$. Typically the set $\mathcal{P}$ is described via the limits on engine speed $\omega_{\text{e,min/max}}$ and the two functions for minimum and maximum engine torque $\tau_{\text{e,min/max}}(\omega_{\text{e}})$, i.e.,

$$\mathcal{P} := \big\{(\omega_{\text{e}}, \tau_{\text{e}}) \in \mathbb{R}^2 : \omega_{\text{e}} \in [\omega_{\text{e,min}}, \omega_{\text{e,max}}] \ \wedge \ \tau_{\text{e}} \in [\tau_{\text{e,min}}(\omega_{\text{e}}), \tau_{\text{e,max}}(\omega_{\text{e}})]\big\}. \tag{18}$$

As an example, the maps experimentally found for our case study are illustrated in Figure 1, where the engine operation domain $\mathcal{P}$ is shown with a black line.

C. Continuous time domain vehicle model

Combining the presented models of all components leads to the complete continuous time domain dynamical model of the vehicle. The inputs are given by engine torque, braking torque and gear shift command, that is $u = [\tau_\mathrm{e}, \tau_\mathrm{b}, u_\mathrm{g}]^\top$. The state is given by vehicle position, velocity and gear number $x(t) = [s(t), v(t), j(t)]^\top$, so that

$$\dot{s}(t) = v(t) \tag{19}$$
$$\dot{v}(t) = a_\mathrm{x}(s(t), v(t), j(t), \tau_\mathrm{e}(t), \tau_\mathrm{b}(t)) \tag{20}$$
$$j^+(t) = j(t) + u_\mathrm{g}(t), \quad \forall t : u_\mathrm{g}(t) \neq 0, \tag{21}$$

where the longitudinal acceleration a_x is given by

$$a_\mathrm{x}(s, v, j, \tau_\mathrm{e}, \tau_\mathrm{b}) = \frac{1}{m_\mathrm{eff}} \left(\frac{\eta^{\mathrm{sign}(\tau_\mathrm{e})\gamma^{(j)}} \tau_\mathrm{e} - \tau_\mathrm{b}}{r} - F_\mathrm{r}(s, v) \right). \tag{22}$$

Although the system dynamics are hybrid (including continuous time and jumping states) we represent the time dynamics through a time independent function $\dot{x} = f_\mathrm{veh}(x, u)$, having as outputs the rotational speed of the engine ω_e, lateral acceleration a_y, fuel consumption rate q_fuel, and $\mathrm{NO_x}$ emission rate $q_{\mathrm{NO_x}}$.

D. Adopted model

For the special case of the vehicle moving only forward, that is $v(t) > 0 \quad \forall t \in [t_0, t_\mathrm{f}]$, the independent variable can be switched from time t to position on the road s. Hence, the number of states is reduced by one, since now the position is the independent variable. Discretizing the vehicle dynamics into a grid $s_k \in \{s_0, s_1, \ldots, s_N\}$, and using the forward Euler method, we find the discrete distance domain representation

$$\begin{aligned} v_{k+1} &= v_k + \tfrac{1}{v_k} a_\mathrm{x}(s_k, v_k, j_k, \tau_{\mathrm{e},k}, \tau_{\mathrm{b},k}) \Delta s_k \\ j_{k+1} &= j_k + u_{j,k}, \end{aligned} \tag{23}$$

where discrete variables are represented with a subscript k and $\Delta s_k = s_{k+1} - s_k$. This dynamics is shortly referred to as $x_{k+1} = f^s_\mathrm{veh}(x_k, u_k, k)$.

E. Emission aware optimal vehicle ecodriving control

In ecodriving the task is typically to control the vehicle such that it moves optimally from a starting position s_0 to a destination s_f, while respecting constraints. The considered constraints are usually given due to system limits, e.g., speed limits, curves, road grade and comfort issue. In this work we refer to emission aware ecodriving as the goal of improving vehicle energy efficiency through manipulating the longitudinal dynamics, also taking into account a constraint on the total $\mathrm{NO_x}$ emissions. Note that the relationship between fuel economy and $\mathrm{NO_x}$ emission rate is not necessarily constant over all the operating range. In fact, it depends mostly on the engine calibration, and our approach is able to exploit these differences. Before introducing the solved emission aware OCP, we introduce the related Emission Constrained Ecodriving Control Problem (EC-ECP) [26], i.e.,

$$\begin{aligned} \min_{x,u} \; & \int_{t_0}^{t_\mathrm{f}} q_\mathrm{fuel}(\omega_\mathrm{e}(v(t), j(t)), \tau_\mathrm{e}(t)) \mathrm{d}t \\ \text{s.t.} \quad & \left. \begin{aligned} \dot{x}(t) &= f_\mathrm{veh}(x(t), u(t)) \\ (x(t), u(t)) &\in \mathcal{C}_\mathrm{ed} \end{aligned} \right\}, \quad \forall t \in [t_0, t_\mathrm{f}] \\ & \#_\mathrm{GS} \leq N_{\mathrm{gs,max}} \\ & m_{\mathrm{NO_x}} \leq m_{\mathrm{NO_x,max}} \\ & s(t_\mathrm{f}) = s_\mathrm{f}, \end{aligned} \tag{EC-ECP}$$

where the objective function is the accumulated fuel consumption $m_\mathrm{fuel} = \int_{t_0}^{t_\mathrm{f}} q_\mathrm{fuel}(\omega_\mathrm{e}(v(t), j(t)), \tau_\mathrm{e}(t)) \mathrm{d}t$. For the sake of simplicity, in (EC-ECP) the pointwise constraints are compactly defined as $\mathcal{C}_\mathrm{ed}$. More specifically, velocity limits, to keep the velocity in the allowed region are defined as

$$v \leq v_\mathrm{max}(s), \tag{24}$$

while engine limits, to keep the engine operating in its normal region, are

$$(\omega_\mathrm{e}(v, j), \tau_\mathrm{e}) \in \mathcal{P}. \tag{25}$$

As for acceleration limits to keep the vehicle operating in comfortable range of accelerations, they are given by

$$(a_\mathrm{x}(s, v, j, \tau_\mathrm{e}, \tau_\mathrm{b}), a_\mathrm{y}(s, v)) \in \mathcal{A}, \tag{26}$$

with the acceleration set defined as

$$\mathcal{A} := \left\{ (a_\mathrm{x}, a_\mathrm{y}) \in \mathbb{R}^2 : A \cdot \begin{bmatrix} a_\mathrm{x} & a_\mathrm{y} \end{bmatrix}^\top \leq \mathbb{1} \right\}, \tag{27}$$

where $\mathbb{1}$ is a vector with all ones and

$$A = \begin{bmatrix} \frac{1}{a_{\mathrm{x,min}}} & \frac{1}{a_{\mathrm{y,min}}} \\ \frac{1}{a_{\mathrm{x,min}}} & \frac{1}{a_{\mathrm{y,max}}} \\ \frac{1}{a_{\mathrm{x,max}}} & \frac{1}{a_{\mathrm{y,min}}} \\ \frac{1}{a_{\mathrm{x,max}}} & \frac{1}{a_{\mathrm{y,max}}} \end{bmatrix}. \tag{28}$$

It is well known in the literature that human drivers are sensitive to the accelerations experienced while driving [40], and they avoid simultaneous high longitudinal and lateral accelerations, thus leading to the typically diamond shaped distribution illustrated in Figure 2. Finally, the domain con-

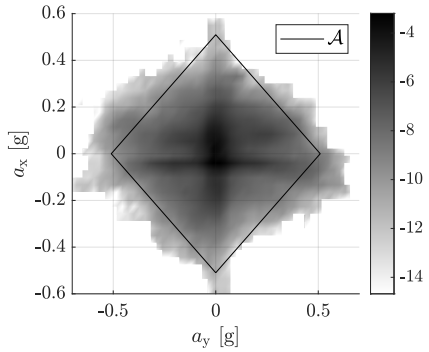

Figure 2: Logarithmic relative frequency of accelerations in measured data to show the human acceptance of acceleration.

straints for braking torque, gear signal and gear change signal are

$$\tau_{\mathrm{b}} \in [0, \tau_{\mathrm{b,max}}] \tag{29}$$
$$j \in \{1, \dots, N_j\} \tag{30}$$
$$u_{\mathrm{g}} \in \{-1, 0, 1\}. \tag{31}$$

The terminal constraint is the final position s_{f} reached at final time t_{f}. The constraint $\#_{\mathrm{GS}} \leq N_{\mathrm{gs,max}}$ is present to avoid the so-called gear hunting phenomena, while the total amount of $\mathrm{NO_x}$ emissions, that is $m_{\mathrm{NO_x}} = \int_{t_0}^{t_{\mathrm{f}}} q_{\mathrm{NO_x}}(\omega_{\mathrm{e}}(v(t), j(t)), \tau_{\mathrm{e}}(t))\mathrm{d}t$, has to stay below the target value $m_{\mathrm{NO_x,max}}$. Note that the problem (EC-ECP) is instrumental to the reasoning underlying the formulation of the solved Emission Aware Ecodriving Control Problem (EA-ECP).

IV. The Proposed Emission Aware Switching NMPC

In this section we present a novel NMPC approach for vehicle ecodriving. It is important to note that the problem (EC-ECP) does not have an explicit time dependency in any of the present terms. Therefore, the problem can be transformed into spatial coordinates by assuming $v > 0$, using the Dirac impulses δ and the relation $\mathrm{d}t = \frac{1}{v}\mathrm{d}s$, that is

$$\min_{u,x} \int_{s_0}^{s_{\mathrm{f}}} \frac{1}{v(s)} q_{\mathrm{fuel}}(\omega_{\mathrm{e}}(v(s), j(s)), \tau_{\mathrm{e}}(s))\mathrm{d}s$$
$$\text{s.t.} \quad \left.\begin{array}{r} \frac{\mathrm{d}x}{\mathrm{d}s}(s) = \frac{1}{v(s)} f_{\mathrm{veh}}(x(s), u(s), s) \\ (x(s), u(s), s) \in \mathcal{C}_{\mathrm{ed}} \end{array}\right\}, \forall s \in [s_0, s_{\mathrm{f}}]$$
$$\int_{s_0}^{s_{\mathrm{f}}} \Big| \sum_{\hat{t} \in T_j} u_{\mathrm{g}}(t) \cdot \delta(t - \hat{t}) \Big| \mathrm{d}s \leq N_{\mathrm{gs,max}} \quad \text{(EA-ECPs)}$$
$$\int_{s_0}^{s_{\mathrm{f}}} \frac{1}{v(s)} q_{\mathrm{NO_x}}(\omega_{\mathrm{e}}(v(s), j(s)), \tau_{\mathrm{e}}(s))\mathrm{d}s \leq m_{\mathrm{NO_x,max}}$$
$$t_0 + \int_{s_0}^{s_{\mathrm{f}}} \frac{1}{v(s)} \mathrm{d}s = t_{\mathrm{f}}.$$

In the space domain the problem depends on the independent variable s. Applying the transformation leads to the new state vector $x(s) = [v(s), j(s)]^\top$. Furthermore the final position constraint $s(t_{\mathrm{f}})$ is s_{f} transformed into a constraint on the total travel time, introducing an isoperimetric constraint.

Since NMPC is applied to discrete problems, considering the grid $s_k \in \{s_0, \dots, s_N\}$, where $s_N = s_{\mathrm{f}}$, the discretized problem using forward Euler method is given by

$$\min_{x,u} \sum_{k=0}^{N-1} \frac{\Delta s_k}{v_k} q_{\mathrm{fuel}}(\omega_{\mathrm{e}}(v_k, j_k), \tau_{\mathrm{e},k})$$
$$\text{s.t.} \quad \left.\begin{array}{r} x_{k+1} = f^s_{\mathrm{veh}}(x_k, u_k, k) \\ (x_k, u_k, k) \in \mathcal{C}_{\mathrm{ed}} \end{array}\right\}, \forall k \in \{0, \dots, N-1\}$$
$$\sum_{k=0}^{N-1} |u_{j,k}| \leq N_{\mathrm{gs,max}}$$
$$\sum_{k=0}^{N-1} \frac{\Delta s_k}{v_k} q_{\mathrm{NO_x}}(\omega_{\mathrm{e}}(v_k, j_k), \tau_{\mathrm{e},k}) \leq m_{\mathrm{NO_x,max}}$$
$$\sum_{k=0}^{N-1} \frac{\Delta s_k}{v_k} = t_{\mathrm{f}} - t_0.$$

(EA-ECPsd)

Since isoperimetric constraints can be dualized into the objective function introducing a weight factor for each constraint, the total number of gearshifts is dualized using μ_{gs}, the emission constraint using $\mu_{\mathrm{NO_x}}$, and the travel time constraint is dualized with $\mu_{t_{\mathrm{f}}}$. Omitting arguments of functions for sake of readability, we write the discrete space domain problem with dualized constraints as

$$\min_{x,u} \sum_{p \in \mathcal{K}_k} \frac{\Delta s_p}{v_p} \left(q_{\mathrm{fuel}}(\cdot) + \mu_{\mathrm{NO_x}} q_{\mathrm{NO_x}}(\cdot) + \mu_{t_{\mathrm{f}}}\right) + \mu_{\mathrm{gs}} |u_{\mathrm{g},p}|$$
$$\text{s.t.} \quad \left.\begin{array}{r} x_{p+1} = f^s_{\mathrm{veh}}(x_p, u_p, p) \\ (x_p, u_p, p) \in \mathcal{C}_{\mathrm{ed}} \end{array}\right\}, \forall p \in \mathcal{K}_k.$$

(EA-ECP)

The new running cost contains the left hand side of the isoperimetric constraints, and the factors $\mu_{\mathrm{NO_x}}$, μ_{gs} and $\mu_{t_{\mathrm{f}}}$. Similar reformulations can be found in [41] for the emission constraint and [19] for the final time constraint. We want to stress that the proposal has the merit to allow in practice to reformulate the more complex emission constrained control problem into a simpler emission aware control problem, by operating a suitable constraint-softening. Note also that the key difficulty in solving (EA-ECP) via traditional NMPC is given by the non-convex and non differentiable nature of the optimization problem. This spurred us to find a valid alternative based on the switching formulation of the problem.

A. The switching vehicle model

Motivated by the fact that under suitable assumptions the optimal operation of a conventional vehicle can be described by a combination of $m_{\mathrm{m}} = 4$ operating modes (acceleration, cruising, coasting, braking, see [13]), we model the vehicle dynamics as a switched system, switching among these four operating modes. Additionally, gear shifting among neighbouring gears can be modelled as operating among three conditions, $u_{\mathrm{g}} = \{-1, 0, 1\}$, therefore leading to switched systems with a total of $M = 12$ possible modes of operation. Specifically, modes $\{1, 2, 3\}$ refers to acceleration, $\{4, 5, 6\}$ to cruising, $\{7, 8, 9\}$ to coasting, and $\{10, 11, 12\}$ to braking, respectively.

Given $\sigma_k \in \{1, \dots, 12\}$, the mode of operation is realized based on the following control laws for the input variables

$$u_{\mathrm{g}}(x_k, \sigma_k, k) = \begin{cases} +1, & \sigma_k \in \{1, 4, 7, 10\} \\ 0, & \sigma_k \in \{2, 5, 8, 11\} \\ -1, & \sigma_k \in \{3, 6, 9, 12\} \end{cases} \tag{32}$$

$$\tau_{\mathrm{e}}(x_k, \sigma_k, k) = \begin{cases} \tau_{\mathrm{e,max}}(x_k, k), & \sigma_k \in \{1, 2, 3\} \\ \tau_{\mathrm{e,cruise}}(x_k, k), & \sigma_k \in \{4, 5, 6\} \\ \tau_{\mathrm{e,min}}(x_k, k), & \sigma_k \in \{7, 8, 9\} \\ \tau_{\mathrm{e,min}}(x_k, k), & \sigma_k \in \{10, 11, 12\} \end{cases} \tag{33}$$

$$\tau_{\mathrm{b}}(x_k, \sigma_k, k) = \begin{cases} 0, & \sigma_k \in \{1, 2, 3\} \\ F_{\mathrm{b,cruise}}(x_k, k), & \sigma_k \in \{4, 5, 6\} \\ 0, & \sigma_k \in \{7, 8, 9\} \\ F_{\mathrm{b,max}}(x_k, k), & \sigma_k \in \{10, 11, 12\}, \end{cases} \tag{34}$$

where $\tau_{\mathrm{e,max}}(x_k, k)$ is the maximum engine torque compatible with the constraints $\mathcal{P}$ and $\mathcal{A}$. The maximum engine torque, $\tau_{\mathrm{e,cruise}}(x_k, k)$, as well as $F_{\mathrm{b,cruise}}(x_k, k)$ are the engine torque and braking force leading to constant speed. As for $\tau_{\mathrm{e,min}}(x_k, k)$, it is the minimum engine torque, and

$F_{\mathrm{b,max}}(x_k,k)$ is the maximum braking force. These values are not constant, but as highlighted before, they are computed at each time such that they comply with the constraint sets $\mathcal{P}$ and $\mathcal{A}$, and such that the velocity v may not overcome $v_{\max}$ in the next step. Furthermore, in all the modes where there could be a simultaneous use of brake force and engine torque, their computation is done in such a way that braking is not used before the engine torque is reduced to the minimum possible value. Note that another important aspect in the ecodriving problem is that of comfort, in order to ensure the adequate speed profiles from the passengers. The latter is implicitly ensured by the control sequences selected according to the ecodriving style. Letting $u_{\sigma_k}(x_k,k) = [\tau_{\mathrm{e}}(x_k,\sigma_k,k), \tau_{\mathrm{b}}(x_k,\sigma_k,k), u_{\mathrm{g}}(x_k,\sigma_k,k)]^\top$ be the input of the discrete vehicle model (23), it becomes evident that the controlled vector field can be written as

$$f_{\sigma_k}(x_k,k) = f^s_{\mathrm{veh}}(x_k, u_{\sigma_k}(x_k,k), k). \tag{35}$$

Now we are in a position to formulate the problem exactly as stated in Section II. In fact, in the considered case we set $h(\cdot)=0$, $g_{\sigma_k}(\cdot)$ as the cost in (SFHOCP), $\mathcal{X}$ as the constraints, and $\mathcal{X}_{\mathrm{f}}$ unused. Note that, the mode-based model (35) can also be used to setup a complete OCP that is solvable by DP.

As baselines, from here on, relying on the problem formulation in (EA-ECP) solved via DP, hence with full horizon (that is considering all the trip window) and restriction of the input to the selected modes, we will refer to it as EDPm (that is Emission aware DP with modes) approach. As mentioned before, in order to solve these DP algorithms, we use the entire trip horizon taking advantage of Bellman's principle of optimality. In fact, using DP with finite horizon could be faster, but it results significantly sensitive to state and input space discretization.

B. Improvements to the NMPC

In our proposed solution we improve the NMPC performance through the following three modifications.

1) Blocking mechanism: The cardinality of $\mathcal{W}_k$, which is strictly related to the computational complexity of solving the NMPC problem, is given by $\mathrm{card}(\mathcal{W}_k) = M^{N_{\mathrm{p}}}$. Due to the exponential growth, this number can become prohibitively large for long prediction horizon, therefore the common blocking strategy is hereafter adopted. Specifically, in its classical version, it consists of fixing the input to be constant over a certain number of steps, thus reducing the number of optimization variables (see [42] for further details). Letting N_{b} be the number of blocks used over the horizon, the new cardinality becomes $\mathrm{card}(\mathcal{W}_k) = M^{N_{\mathrm{b}}}$.

2) Gear shifting strategy: Since complexity reduction achieved by blocking maybe not sufficient, the following simplified gear shift logic is adopted. Specifically, we only allow a controlled gear shift at the first prediction step, while an auxiliary gear shift control law $\bar{u}_j$ is used afterwards:

$$u_{\mathrm{g}}(x_p,\sigma_p,p) = \begin{cases} u_{\mathrm{g}}(x_p,\sigma_p,p), & p=k \\ \bar{u}_j(x_p,p), & p\neq k. \end{cases} \tag{36}$$

The auxiliary law is defined as

$$\bar{u}_j(x_p,p) = \begin{cases} +1, & \omega_{e,p+1} > \omega_{\mathrm{e,max}} \\ -1, & \omega_{e,p+1} < \omega_{\mathrm{e,min}} \\ 0, & \text{otherwise.} \end{cases} \tag{37}$$

This strategy further reduces the cardinality of $\mathcal{W}_k$ to $\mathrm{card}(\mathcal{W}_k) = M \cdot m_{\mathrm{m}}^{(N_{\mathrm{b}}-1)} = 12 \cdot 4^{(N_{\mathrm{b}}-1)}$.

3) Velocity limit precomputation: Having in mind the field implementation of the proposed strategy, it is especially helpful to use short prediction horizons. However, in this case the presence of curves, which can only be driven with a certain maximum speed, could not immediately appear in the selected prediction window. Therefore, the feasibility of the optimization within NMPC algorithm can be improved for small horizons by introducing an improved velocity limit $\bar{v}_{\max}$. The latter is used instead of the limit given by the route properties, originally indicated as $v_{\max}$. The improved velocity limit $\bar{v}_{\max}$, now used inside the previous switching NMPC algorithm, can be computed relying on a minimum time solution to a simplified problem. This problem is instrumental to ensure the feasibility of the proposed approach, and since it is a relaxation of the original ecodriving problem, the solution is guaranteed to be fast and therefore it can be used as a less conservative limit.

The considered reduced space domain system dynamics is

$$\tfrac{\mathrm{d}}{\mathrm{d}s}v(s) = \tfrac{1}{v(s)}a_{\mathrm{x}}(s). \tag{38}$$

On a route with curvature $c(s)$ the lateral acceleration is given by $a_{\mathrm{y}}(s) = v^2(s)\cdot c(s)$. If we would consider v and s as the state variables, the above equation is clearly a nonlinear relation, but if we formulate the problem over space and define $x = v^2$ the system turns out to be linear and the problem becomes convex. The state transformation $x = v^2$ is only possible if we assume $v > 0$, but this assumptions is clearly valid for minimum time solutions. Using the relations $\mathrm{d}t = \frac{1}{v}\mathrm{d}s, u = a_{\mathrm{x}}, x = v^2$ we see that

$$\frac{\mathrm{d}x}{\mathrm{d}s}(s) = 2v(s)\frac{\mathrm{d}v}{\mathrm{d}s}(s) = 2v(s)\frac{1}{v(s)}a_{\mathrm{x}}(s) \tag{39}$$

$$\frac{\mathrm{d}x}{\mathrm{d}s}(s) = 2u(s), \tag{40}$$

and $a_{\mathrm{y}}(s) = x(s)\cdot c(s)$. So the differential equation (40) is linear and the lateral acceleration is a linear function in state and input. Hence, the acceleration constraint minimum time solution can be found by solving the following convex problem

$$\begin{aligned} \min_{u(s),x_0} & \int_{s_0}^{s_f} \frac{1}{\sqrt{x(s)}}\mathrm{d}s \\ \text{s.t.} \quad & \tfrac{\mathrm{d}}{\mathrm{d}s}x(s) = 2u(s) \qquad\qquad x(0) = x_0 \\ & x(s) \leq v^2_{\max}(s) \quad A\cdot\begin{bmatrix} u(s) \\ c(s)\cdot x(s)\end{bmatrix} \leq \mathbb{1} \end{aligned}, \tag{41}$$

with A as in (28). Due to the convexity of the problem (41) it can be solved efficiently by discretizing the spatial domain and performing numerical optimization. It is worth to highlight that such precomputation involves only the acceleration bounds, which are rather standard to comply with comfort requirements, and the a priori known road parameters. Therefore, the

proposed add-on to the switching NMPC not only does not need to be performed online, but it is also independent of the vehicle parameters, thus resulting generally applicable on the field.

Finally, the formulation of the solved Switching Emission Aware Ecodriving Control Problem (SEA-ECP) becomes

$$\min_{\mathbf{w}_k} \sum_{p\in\mathcal{K}_k} \frac{\Delta s_p}{v_p}\left(q_{\text{fuel}} + \mu_{\text{NO}_\text{x}} q_{\text{NO}_\text{x}} + \mu_{t_\text{f}}\right) + \mu_{\text{gs}}|u_{\text{g}}(x_p, \sigma_b, p)|$$
$$\text{s.t.} \quad \left.\begin{array}{l} x_{p+1|k} = f^s_{\text{veh}}(x_{p|k}, \nu_{p|k}, p) \\ (p, x_{p|k}, \nu_{p|k}) \in \overline{\mathcal{C}}_{\text{ed}} \end{array}\right\}, \forall p \in \mathcal{K}_k, \tag{SEA-ECP}$$

with initial state $x_{k|k} = x_k$, $\nu_{p|k} = u_{\sigma_{b|k}}(x_p, p)$, where $b = \lfloor \frac{p}{B} \rfloor$, with B being the block size, and $N_\text{p} = N_\text{b} \cdot B$ being the used prediction horizon. The new set of constraint $\overline{\mathcal{C}}_{\text{ed}}$ instead includes

$$v \leq \bar{v}_{\max}, \tag{42}$$

with (25), (26), (29), (30),(31), and using (36) and (37).

V. Case Study

The results presented hereafter are generated based on real data and settings reported in [33]. The used route parameters are based on a trip from Johannes Kepler University (JKU) Linz to Altenberg, a nearby village, and back. The route has a length of 12 km, a maximum altitude of 380 m above start and seven curves with radius smaller than 50 m. For this study of the control performance, the vehicle starts at position $s_0 = 0$ and shall drive until $s_\text{f} = 12\,\text{km}$. The initial state is set to $v_0 = 10\,\text{m/s}$, $j_0 = 4$.

A. Performance of the proposed SNMPC

As for the impact of the restriction to modes, the performance of the proposed SNMPC accounting emissions is comparable to that in [34], with Pareto fronts in terms of t_f and m_{fuel} closer to the optimal ones achieved via EDPm, higher the horizon is. The discretization parameters used to solve the optimal control problem through EDPm are given in Table II. The input is assumed to be discrete as given in Section IV.

Table II: Discretization parameters for EDPm.

Variable	min	max	steps	Δ
v [km/h]	1	100	100	1
j [1]	1	8	8	1
s [m]	0	12000	2401	5

Figure 3 illustrates the time evolution of the velocity, gear shifting, fuel consumption, and NO_x emission when using the SNMPC with $N_\text{p} = 20$, $N_\text{b} = 4$ and different cost function weights, tuned according to a trial and error procedure. It can be observed that the SNMPC fulfills all the constraints in terms of velocity limits and curving speed, while maintaining limited the level of fuel consumption, gear shifting and NO_x emission, consistently to the dualization operated in the emission aware control problem.

The computational complexity of the SNMPC, that is important for real implementation, is also evaluated. Since the

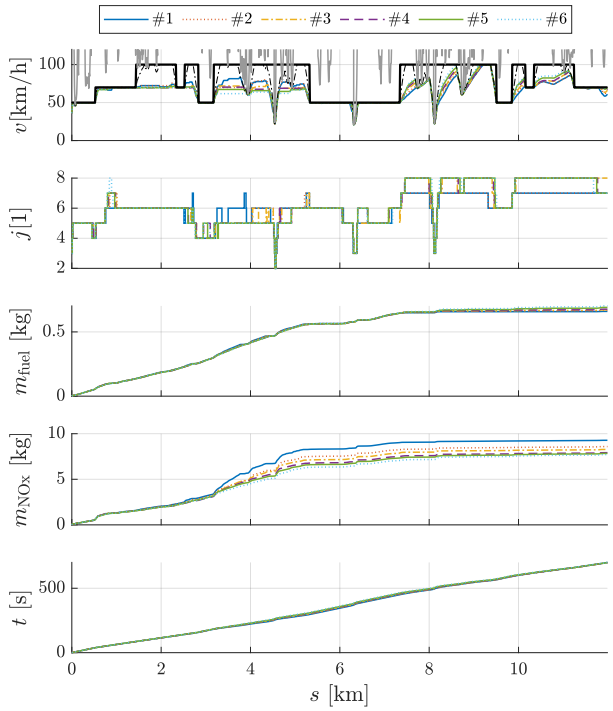

Figure 3: Time series of speed, gear shifting, fuel consumption and NO_x emission, when using the SNMPC with $N_\text{p} = 20$, $N_\text{b} = 4$, and settings as in Table IV.

computation time t_{comp} is not constant over time, we compute the average and standard deviation of t_{comp} for various settings on a workstation computer with an Intel i5-6400 CPU with 2.7 GHz and 16 GB RAM, see Table III. In particular, the value N_b plays a crucial role and, after a sensitivity study, the most significant choices for field implementations are indicated. Clearly, as expected, the computation time rises with

Table III: Dependency of computation time on the parameters N_b and N_p with weights $\mu_{t_\text{f}} = 0.005$, $\mu_{\text{gs}} = 0.00022$, [34].

	t_{comp} [ms]			
	N_p			
N_b	10	20	30	40
3	6.3 ± 1.79	12.7 ± 3.70	16.7 ± 2.10	22.1 ± 1.56
4	8.6 ± 0.35	17.1 ± 2.48	23.1 ± 2.26	29.9 ± 3.80
5	24.1 ± 2.59	41.6 ± 10.57	49.7 ± 9.81	60.1 ± 11.53
6	81.3 ± 13.45	130.9 ± 29.52	167.4 ± 37.59	191.7 ± 43.32

both higher N_p and N_b. Yet, even with the most demanding settings, the average computation time for the SNMPC is below 0.2 s, which is smaller with respect to the one in case of a NMPC solved via DP with modes, that is 0.25 s. Note that, differently from DP, as previously mentioned, our proposal could be further sped up via parallelization. Indeed, it allows to linearly scale the algorithm computations in Table III with the number of cores.

B. Emission aware performance

Now we analyze the trade-off NO_x versus fuel, represented by m_{NO_x} and m_{fuel}. All the results are reported in Table IV.

Note that the weight μ_{gs} is selected in order to have a number of gearshifts similar to the ones measured on the vehicle on the same route. Figure 4 shows five Pareto curves, one for the EDPm solution, as an optimal baseline, and four related to the SNMPC. The latter are not smooth and do not show a clear trend when the prediction horizon is changed. Interestingly, it seems that for $N_b = 4$ the settings $N_p = 20$ performs best. Note that the shape of the Pareto fronts, especially for $N_p = \{20, 30, 40\}$, are very similar to the DP solution, and the offset in fuel is less than $3\,\%$. Moreover, the NO_x emission can be influenced in almost the same range as for the global optimal solution.

Table IV: Control performances using SNMPC with $N_{\text{b}} = 4$.

N_{p}	#	m_{fuel}[kg]	m_{NO_x} [g]	t_{f} [s]	#GS[1]	$\mu_{t_{\text{f}}}$ [-]	μ_{gs} [-]	μ_{NO_x} [-]
10	1	0.678	9.188	699.6	48	7.0e-03	1.5e-04	0.0e+00
	2	0.679	7.845	699.9	47	9.2e-03	2.0e-04	1.0e-02
	3	0.687	7.788	700.8	44	1.2e-02	3.5e-04	2.0e-02
	4	0.695	7.598	700.9	46	1.6e-02	4.2e-04	4.0e-02
	5	0.714	7.631	699.9	56	3.4e-02	4.8e-04	1.0e-01
20	1	0.660	9.278	700.5	46	2.9e-03	3.5e-04	0.0e+00
	2	0.667	8.589	699.2	40	3.8e-03	3.0e-04	4.0e-03
	3	0.671	8.273	699.1	56	4.8e-03	3.7e-04	1.0e-02
	4	0.677	7.920	699.0	48	6.1e-03	4.0e-04	2.0e-02
	5	0.691	7.838	699.2	50	1.0e-02	4.2e-04	4.0e-02
	6	0.702	7.710	700.8	50	2.0e-02	4.8e-04	1.0e-01
30	1	0.663	9.856	700.6	51	2.2e-03	7.3e-04	0.0e+00
	2	0.669	9.277	700.8	48	3.2e-03	7.3e-04	1.0e-02
	3	0.677	8.369	700.4	50	4.9e-03	8.0e-04	2.0e-02
	4	0.684	8.121	700.3	52	6.4e-03	8.0e-04	3.0e-02
	5	0.690	8.031	699.0	54	8.0e-03	8.5e-04	4.0e-02
	6	0.702	7.869	699.2	56	1.6e-02	9.5e-04	1.0e-01
	7	0.714	7.803	700.5	46	1.3e+00	1.1e-01	1.0e+01
40	1	0.664	10.184	700.8	67	1.7e-03	7.3e-04	0.0e+00
	2	0.670	9.045	698.9	56	3.1e-03	7.3e-04	1.0e-02
	3	0.675	8.402	700.7	58	4.4e-03	8.0e-04	2.0e-02
	4	0.684	8.243	699.4	56	5.8e-03	8.0e-04	3.0e-02
	5	0.710	7.864	701.2	48	1.1e+00	1.1e-01	1.0e+01

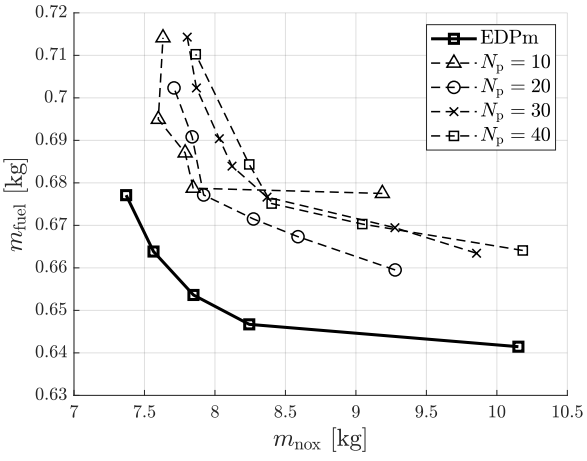

Figure 4: Comparison of Pareto fronts between EDPm and-SNMPC with $N_{\text{b}} = 4$ and $N_{\text{p}} \in \{10, 20, 30, 40\}$.

So it can be concluded that, the proposal is able to realize emission aware driving and influences the achieved emissions in a wide range. Although in the emission aware framework the Pareto fronts do not tend to the one of EDPm solution, as much as it instead occurs when only fuel consumption is minimized (see [34]), it is worth to put the attention on the fact that the offset is very small.

VI. Concluding remarks

The paper has proposed a novel approach based on NMPC applied to the ecodriving control problem, where gear shifting and longitudinal dynamics are controlled. The vehicle model is described as the combination of specific operating modes, which enable the use of a special version of NMPC of switching type. Many studies have shown the potential that optimal control based ecodriving can offer, but these solutions are often difficult to be translated into online control strategies, due to the complexity of the optimal control problem and therefore to the computational burden. If on the one hand the optimal solution, i.e., DP approach, still guarantees good perfomance, on the other hand it has been shown that our solution can operate in real time, while recovering most of the performance achievable by an offline optimal solution for the ecodriving control problem. Albeit a natural slightly decrease in performance is observed with respect to DP, we have proposed a valid ready-to-implement alternative to ecodriving control. Furthermore, differently from DP, our switching NMPC does not suffer the curse of dimensionality, meaning that it can be extended to more complex models without a big impact on the execution time.

Although only the common case of NO_x emission rate in steady-state has been addressed, the presented ideas appear to be extendable to more general settings. For example, it extends to other dynamic emission models, such as particulate matter (PM) or hydrocarbons (HC). Less immediate extensions, where emissions generated during the transient operation are directly considered, are currently under investigation.

Appendix A
Model Parametrization

In this appendix the parametrization of the mathematical vehicle model previously described is presented.

A. Data Acquisition

The car used for data acquisition is described in Table V and shown in Figure 5. As for the emission measurement, since the

Figure 5: The profile view of the test car with portable emission measurement system (PEMS), [43].

exhaust gas components $c \in \{\text{N}_2, \text{O}_2, \text{CO}_2, \text{CO}, \text{NO}, \text{NO}_2\}$ are measured as a volume fraction $x_c \in [0, 1]$ but we are interested in the mass flow q_c, a conversion is necessary. The

Table V: Instrumented vehicle for on-road data acquisition, which is the vehicle to be modelled.

Manufacturer	BMW
Vehicle type	320d (Efficient Dynamics)
Model year	2012
Gearbox	8 Gear AT, ZF8HP
Engine type	CI Diesel (N47)
Engine Size	2 L
$T_{\max}$	380 Nm
$P_{\max}$	120 kW(163 PS)
Emission standard	EURO 5
Emission aftertreatment	DPF, EGR

conversion can be done based on the assumption that the composition of the exhaust gas (in terms of volume fractions) is known and a measurement for the exhaust gas mass flow q_{exh} is available, see [44] for details. From the measured composition the molar mass of the exhaust gas M_{exh} can be computed as $M_{\text{exh}} = \sum_c x_c \cdot M_c$, where x_c are the considered gas components and M_c the molar masses for each of the components. Once M_{exh} is known, q_{NO_x} can be computed as

$$q_{\text{NO}} = x_{\text{NO}} \cdot \frac{M_{\text{NO}}}{M_{\text{exh}}} \cdot q_{\text{exh}} \tag{43}$$

$$q_{\text{NO}_2} = x_{\text{NO}_2} \cdot \frac{M_{\text{NO}_2}}{M_{\text{exh}}} \cdot q_{\text{exh}}, \tag{44}$$

and $q_{\text{NO}_\text{x}} = q_{\text{NO}} + q_{\text{NO}_2}$.

Additionally the time delay introduced by the measurement devices have been analyzed and accounted for by shifting the signals correspondingly. Although the aerodynamic properties are clearly influenced by measurement devices, we argue that the model obtained using this measurement setup still remains representative for a conventional car.

As for the acceleration data from the Altenberg dataset, they can be visualized in the acceleration diagram reported in Figure 2.

B. Vehicle body and power-train model

The found model parameters of the considered vehicle are shown in Table VI.

Table VI: Vehicle and power-train model parameters for the BMW F31 320d Efficient Dynamics (2012) with a ZF8HP 8 Gear automatic transmission.

g	ρ_{air}	m	r	A	c_r	c_d	η
9.81	1.2	1900	0.31	2.2	0.0108	0.263	0.95
[m/s^2]	[kg/m^3]	[kg]	[m]	[m^2]	[1]	[1]	[1]
$\gamma^{(j)}$	[12.06,8.05,5.39,4.27,3.29,2.56,2.15,1.71]						
$\lambda^{(j)}$	[1.3,1.24,1.16,1.1,1.06,1.04,1.02,1]						

C. Road model

To find the functions $\phi(s), c(s), v_{\max}(s)$, the Global Positioning System (GPS) measurements of latitude and longitude are converted into the Universal Transverse Mercator (UTM) coordinate system and the road topology is found as the spatial average of all the measurements. The data and the averaging result are shown in Figure 6. Afterwards the functions $\phi(s)$ and $c(s)$ are extracted from the representation of the road in terms of x_{utm}, y_{utm} and h through finite difference approximation

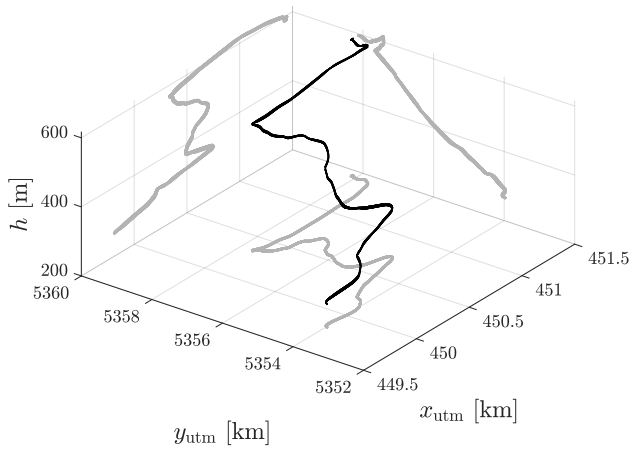

Figure 6: Road topology represented in the three dimensional Universal Transverse Mercator (UTM) coordinate system.

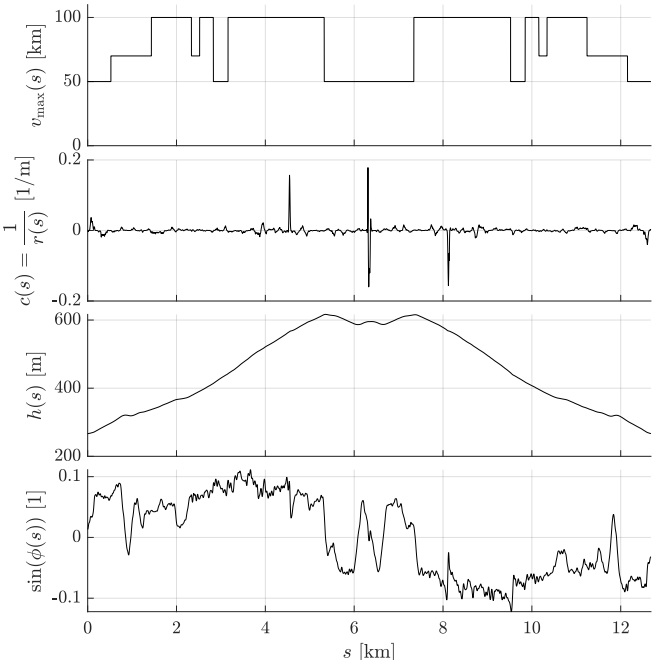

Figure 7: Model of the Altenberg route JKU–Altenberg–JKU, given by speed limit, road grade and curve radius.

of the curvature and grade. The velocity limit signal $v_{\max}(s)$ is extracted from public available OpenStreetMap for the driven road information. The final road model for the route JKU–Altenberg–JKU is shown in Figure 7.

D. Engine model

The engine is described by two nonlinear static functions q_{fuel} and q_{NO_x}, which depend on ω_{e} and τ_{e}. The found maps are illustrated in Figure 1.

Appendix B
Model Validity

We show now the validity of the model by assessing its performance on the retrieved road measurement dataset. Model

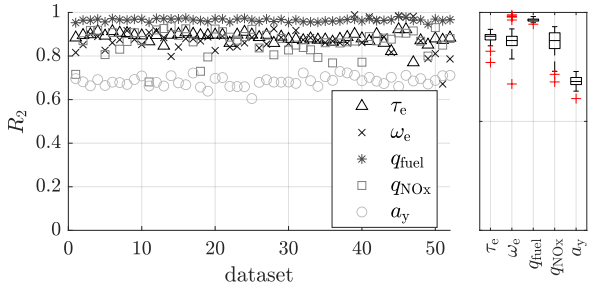

Figure 8: Model performance overview: R_2 value of the model and measured signals is shown for each dataset, and q_{fuel}, q_{NO_x}, τ_e, ω_e, and a_y. The right graph shows a more compact illustration of the information by means of boxplots.

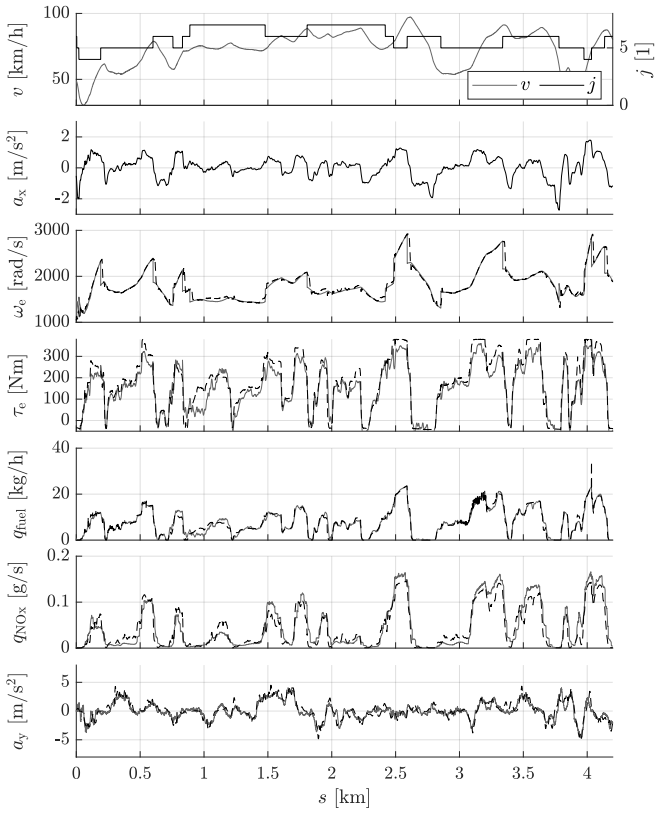

Figure 9: Exemplary performance of the model (black dashed lines) on the first $4.2\,\text{km}$, using backward simulation to reproduce the signals ω_e , τ_e, q_{fuel}, q_{NO_x}, and a_y based on measurements (gray lines).

signals for q_{fuel}, q_{NO_x}, τ_e, ω_e and a_y are computed through backward simulation. The model performance is assessed through R_2 values and exemplary time series plots. In Figure 8 the R_2 value for each model signal on each of the datasets is shown, while, additionally, the results are presented more compactly by means of a boxplot in the right. Although some measurement runs have significant lower performance than others, the models are found to represent the system behaviour very well. In Figure 9 an exemplary comparison, over a subset of the dataset from the Altenberg measurements, is shown for the considered vehicle model.

REFERENCES

[1] B. Brunekreef and S. T. Holgate, "Air pollution and health," *The Lancet*, vol. 360, no. 9341, pp. 1233–1242, Oct. 2002.

[2] K. Zhang and H. C. Frey, "Road grade estimation for on-road vehicle emissions modeling using light detection and ranging data," *Journal of the Air & Waste Management Association*, vol. 56, no. 6, pp. 777–788, 2006.

[3] K. Boriboonsomsin and M. Barth, "Impacts of road grade on fuel consumption and carbon dioxide emissions evidenced by use of advanced navigation systems," *Transportation Research Record*, vol. 2139, no. 1, pp. 21–30, Jan. 2009.

[4] F. J. W. Biegstraaten, J. C. Heemrood, J. Moraal, and M. W. A. Ramackers, "Driving styles in urban areas: how to minimize damage to the environment," Netherlands, Jan. 1985, Ministerie van Volkshuisvesting, Ruimtelijke Ordening en Milieubeheer.

[5] J. N. Barkenbus, "Eco-driving: An overlooked climate change initiative," *Energy Policy*, vol. 38, no. 2, pp. 762–769, Feb. 2010.

[6] M. S. Alam and A. McNabola, "A critical review and assessment of Eco-Driving policy & technology: Benefits & limitations," *Transport Policy*, vol. 35, pp. 42–49, Sep. 2014.

[7] H. Johansson, "Impact of ecodriving on emissions and fuel consumption," *Publication of: Swedish National Road Administration*, 1999.

[8] D. J. Fagnant and K. Kockelman, "Preparing a nation for autonomous vehicles: opportunities, barriers and policy recommendations," *Transportation Research Part A: Policy and Practice*, vol. 77, pp. 167–181, Jul. 2015.

[9] J. Levinson, J. Askeland, J. Becker, J. Dolson, D. Held, S. Kammel, J. Z. Kolter, D. Langer, O. Pink, V. Pratt, M. Sokolsky, G. Stanek, D. Stavens, A. Teichman, M. Werling, and S. Thrun, "Towards fully autonomous driving: Systems and algorithms," in *IEEE Intelligent Vehicles Symposium*, Baden-Baden, Germany, Jun. 2011, pp. 163–168.

[10] H. Farooqi, G. P. Incremona, and P. Colaneri, "Railway collaborative ecodrive via dissension based switching nonlinear model predictive control," *European Journal of Control*, vol. 50, pp. 153–160, Nov. 2019.

[11] S. Aradi, T. Bécsi, and P. Gáspár, "Design of predictive optimization method for energy-efficient operation of trains," in *European Control Conference*, Strasbourg, France, Jun. 2014, pp. 2490–2495.

[12] G. Ribichini and E. Frazzoli, "Efficient coordination of multiple-aircraft systems," in *42nd IEEE International Conference on Decision and Control*, vol. 1, Maui, HI, USA, Dec. 2003, pp. 1035–1040.

[13] A. Sciarretta, G. De Nunzio, and L. L. Ojeda, "Optimal ecodriving control: Energy-efficient driving of road vehicles as an optimal control problem," *IEEE Control Systems*, vol. 35, no. 5, pp. 71–90, Oct. 2015.

[14] D. Moser, H. Waschl, H. Kirchsteiger, R. Schmied, and L. del Re, "Cooperative adaptive cruise control applying stochastic linear model predictive control strategies," in *European Control Conference*, Linz, Austria, Jul. 2015, pp. 3383–3388.

[15] D. Moser, R. Schmied, H. Waschl, and L. del Re, "Flexible spacing adaptive cruise control using stochastic model predictive control," *IEEE Transactions on Control Systems Technology*, vol. 26, no. 1, Jan. 2018.

[16] Q. Jin, G. Wu, K. Boriboonsomsin, and M. J. Barth, "Power-Based Optimal Longitudinal Control for a Connected Eco-Driving System," *IEEE Transactions on Intelligent Transportation Systems*, vol. 17, no. 10, pp. 2900–2910, Oct. 2016.

[17] C. Huang, R. Salehi, and A. G. Stefanopoulou, "Intelligent cruise control of diesel powered vehicles addressing the fuel consumption versus emissions trade-off," in *American Control Conference*, Milwaukee, WI, USA, Jun. 2018, pp. 840–845.

[18] F. Mensing, R. Trigui, and E. Bideaux, "Vehicle trajectory optimization for application in ECO-driving," in *IEEE Vehicle Power and Propulsion Conference*, Chicago, IL, USA, Sep. 2011, pp. 1–6.

[19] E. Hellström, J. Åslund, and L. Nielsen, "Design of an efficient algorithm for fuel-optimal look-ahead control," *Control Engineering Practice*, vol. 18, no. 11, pp. 1318–1327, Nov. 2010.

[20] E. Hellström, M. Ivarsson, J. Åslund, and L. Nielsen, "Look-ahead control for heavy trucks to minimize trip time and fuel consumption," *Control Engineering Practice*, vol. 17, no. 2, pp. 245–254, Feb. 2009.

[21] S. Xu, S. E. Li, X. Zhang, B. Cheng, and H. Peng, "Fuel-optimal cruising strategy for road vehicles with step-gear mechanical transmission," *IEEE Transactions on Intelligent Transportation Systems*, vol. 16, no. 6, pp. 3496–3507, Dec. 2015.

[22] S. Xu, S. E. Li, B. Cheng, and K. Li, "Instantaneous feedback control for a fuel-prioritized vehicle cruising system on highways with a varying slope," *IEEE Transactions on Intelligent Transportation Systems*, vol. 18, no. 5, pp. 1210–1220, May 2017.

[23] H. Chen, L. Guo, H. Ding, Y. Li, and B. Gao, "Real-time predictive cruise control for eco-driving taking into account traffic constraints," *IEEE Transactions on Intelligent Transportation Systems*, vol. 20, no. 8, pp. 2858–2868, Aug. 2019.

[24] S. A. Sajadi-Alamdari, H. Voos, and M. Darouach, "Nonlinear model predictive extended eco-cruise control for battery electric vehicles," in *24th Mediterranean Conference on Control and Automation*, Athens, Greece, Jun. 2016, pp. 467–472.

[25] T. Schwickart, H. Voos, J. R. Hadji-Minaglou, M. Darouach, and A. Rosich, "Design and simulation of a real-time implementable energy-efficient model-predictive cruise controller for electric vehicles," *Journal of the Franklin Institute*, vol. 352, no. 2, pp. 603–625, Feb. 2015.

[26] A. R. Dohner, "Optimal control solution of the automotive emission-constrained minimum fuel problem," *Automatica*, vol. 17, no. 3, pp. 441–458, May 1981.

[27] J. Wang, Q. Yu, S. Li, N. Duan, and K. Li, "Eco speed optimization based on real-time information of road gradient," *Journal Of Automotive Safety And Energy*, vol. 5, no. 03, pp. 257–262, Mar. 2014.

[28] M. Kamal and T. Kawabe, "Eco-driving using real-time optimization," in *European Control Conference*, Linz, Austria, Jun. 2015, pp. 111–116.

[29] A. Bakibillah, M. Kamal, C. Tan, T. Hayakawa, and J. Imura, "Eco-driving on hilly roads using model predictive control," in *7th International Conference on Informatics, Electronics Vision and 2nd International Conference on Imaging, Vision Pattern Recognition*, Kitakyushu, Japan, Jun. 2018, pp. 476–480.

[30] F. Mensing, E. Bideaux, R. Trigui, J. Ribet, and B. Jeanneret, "Eco-driving: An economic or ecologic driving style?" *Transportation Research Part C: Emerging Technologies*, vol. 38, pp. 110–121, Jan. 2014.

[31] J. Deng, P. Polterauer, and L. del Re, "Emission aware eco-driving on country roads," in *ASME 2019 Dynamic Systems and Control Conference*, Park City, Utah, USA, Nov. 2019.

[32] G. Pease, D. Limebeer, and P. Fussey, "Fuel consumption minimization, with emissions constraints, for diesel powered cars," *IEEE Transactions on Control Systems Technology*, vol. 28, no. 4, pp. 1243–1257, Jul. 2020.

[33] P. Polterauer, "Emission aware ecodriving control," Ph.D. dissertation, Institue for Design and Control of mechatronical Systems, Johannes Kepler University Linz, 2019.

[34] P. Polterauer, G. P. Incremona, P. Colaneri, and L. del Re, "A switching nonlinear MPC approach for ecodriving," in *American Control Conference*, Philadelphia, PA, USA, Jul. 2019.

[35] P. Colaneri, J. C. Geromel, and A. Astolfi, "Stabilization of continous-time switiched nonlinear systems," *Systems and Control Letters*, vol. 57, no. 1, pp. 95–103, Jan. 2008.

[36] P. Colaneri and R. Scattolini, "Robust model predictive control of discrete-time switched systems," *IFAC Proceedings Volumes*, vol. 40, no. 14, pp. 208–212, 2007.

[37] L. Zhang, S. Zhuang, and R. D. Braatz, "Switched model predictive control of switched linear systems: feasibility, stability and robustness," *Automatica*, vol. 67, pp. 8–21, May 2016.

[38] M. A. Müller and F. Allgöwer, "Improving performance in model predictive control: Switching cost functionals under average dwell-time," *Automatica*, vol. 48, no. 2, pp. 402–409, Feb. 2012.

[39] L. Guzzella and A. Sciarretta, *Vehicle Propulsion Systems: Introduction to Modeling and Optimization*, 3rd ed. Berlin Heidelberg: Springer-Verlag, 2013.

[40] R. Vaiana, T. Iuele, V. Astarita, M. V. Caruso, A. Tassitani, C. Zaffino, and V. P. Giofrè, "Driving behavior and traffic safety: An acceleration-based safety evaluation procedure for smartphones," *Modern Applied Science*, vol. 8, no. 1, p. 88, Jan. 2014.

[41] S. Zentner, J. Asprion, C. Onder, and L. Guzzella, "An equivalent emission minimization strategy for causal optimal control of diesel engines," *Energies*, vol. 7, no. 3, pp. 1230–1250, Feb. 2014.

[42] R. Cagienard, P. Grieder, E. C. Kerrigan, and M. Morari, "Move blocking strategies in receding horizon control," in *43rd IEEE Conference on Decision and Control*, vol. 2, Atlantis, Paradise Island, Bahamas, Dec. 2004, pp. 2023–2028.

[43] L. Oberguggenberger, "Analysis and Modeling of Real Driving Emissions," Master's thesis, Johannes Kepler University (JKU) Linz, 2017.

[44] J. B. Heywood *et al.*, *Internal combustion engine fundamentals*. Mcgraw-hill New York, 1988.

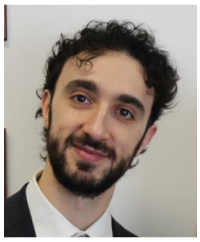

Gian Paolo Incremona (M'12) is Assistant Professor of Automatic Control at Politecnico di Milano, Italy. He was a student of the Almo Collegio Borromeo of Pavia, and of the class of Science and Technology of the Institute for Advanced Studies IUSS of Pavia. He received the Bachelor and Master degrees (with highest honor) in Electric Engineering, and the Ph.D. degree in Electronics, Electric and Computer Engineering from the University of Pavia in 2010, 2012 and 2016, respectively. From October to December 2014, he was with the Dynamics and Control Group at the Eindhoven Technology University, The Netherlands. He was a recipient of the 2018 Best Young Author Paper Award from the Italian Chapter of the *IEEE Control Systems Society*, and he has been a member of the conference editorial boards of the *IEEE Control System Society* and of the *European Control Association*, since 2018. At present, he is *Associate Editor* of the journal *Nonlinear Analysis: Hybrid Systems*, and of the *International Journal of Control*. His research interests include variable structure control, model predictive control, industrial robotics, power systems, transportation systems, and glycemia control in diabetic subjects.

Philipp Polterauer was a research assistant with the Institute for Design and Control of Mechatronical Systems, JKU Linz until 2019 and is currently a development engineer at the MAGNA Engineering Center Steyr. He received the bachelor, master and the Ph.D. degree in mechatronics from JKU Linz, Austria, all with distinction. His current research interests include the modelling and control of vehicles, mainly focusing on improving energy efficiency and emission reduction through applying optimal control.